

Amplifying hybrid entangled states and superpositions of coherent states

InU Jeon, Sungjoo Cho, and Hyunseok Jeong

Department of Physics and Astronomy, Seoul National University, Seoul 08826, Korea

(Dated: September 26, 2024)

We compare two amplification schemes, photon addition and then subtraction ($\hat{a}\hat{a}^\dagger$) and successive photon addition ($\hat{a}^{\dagger 2}$), applied to hybrid entangled states (HESs) and superpositions of coherent states (SCSs). We show that the amplification schemes' fidelity and gain for HESs are the same as those of coherent states. On the other hand, SCSs show quite nontrivial behaviors by the amplification schemes, depending on the amplitudes of coherent states, number of coherent-state components, and relative phases between the components. This implies that appropriate amplification schemes for SCSs should be chosen depending on the tasks and specific forms of the states. To investigate the quality of amplified states, we calculate the quantum Fisher information, a measure of quantum phase estimation. In terms of the quantum Fisher information, the $\hat{a}\hat{a}^\dagger$ scheme tends to show better performance for relatively small amplitudes while the $\hat{a}^{\dagger 2}$ scheme is better in larger amplitude regime. The performance of the two schemes becomes indistinguishable as the amplitude grows sufficiently large.

I. INTRODUCTION

Hybrid entangled states (HESs) [1, 2] and superpositions of coherent states (SCSs) [3, 4] in free-traveling fields are well-known nonclassical states. A HES is an entangled state between a discrete-variable (DV) system such as a photon number state and a continuous-variable (CV) system such as a coherent state. This integrated perspective toward the traditional dichotomy of CV and DV quantum information brings new advantages that could not have been obtained in each area individually. Apart from its theoretical versatility, interplay and conversion between CV and DV systems [5] have been experimentally realized [6–8] indicating generation and processing of hybrid entanglement are well within our reach. HESs are also useful for fundamental studies on quantum physics such as loss-tolerant verification of Bell-inequality violations [9], quantum teleportation [6, 7, 10–13], quantum computation [13, 14], quantum communication [15–17] and steering verification [18, 19]. Generation schemes for HESs were theoretically proposed [1, 2, 20–23] and experimentally implemented [1, 2]. SCSs are superpositions of coherent states with different phases, and a typical example is a superposition of two coherent states with opposite phases. They are useful for many quantum information tasks such as quantum computation [24–29], quantum teleportation [30–32], precision measurements [33–41], non-Gaussian state generation [42–44] and error suppression [45, 46]. They have also been used to investigate violations of local realism [47, 48] and nonlocal realism [49, 50]. SCSs in free-traveling fields have been implemented approximately using various methods [51–56]. In these regards, obtaining sufficiently large amplitudes of continuous variables in HESs or SCSs is required to accomplish various quantum information processing tasks.

One way to obtain HESs or SCSs of large amplitudes is to amplify the states [26, 32, 57–60] or purify them [17, 61]. Although a deterministic noiseless linear amplification for a bosonic system is forbidden by quan-

tum mechanics [62], there have been studies on nondeterministic amplification of coherent states [63–65]. In this paper, we adopt the photon addition and then subtraction scheme [63, 64] ($\hat{a}\hat{a}^\dagger$) and the successive photon addition scheme [65] ($\hat{a}^{\dagger 2}$). We compare the fidelity and gain of the two schemes and take quantum Fisher information *for phase estimation* [66–70] as an indicator for the performance of amplification. This could be a practical measure in estimating the amplification performance because various nonclassical states of light fields are utilized for quantum phase estimation [71–74]. In fact, in a previous work [65], the quantum Fisher information is employed as a measure for amplification schemes using $\hat{a}\hat{a}^\dagger$ and $\hat{a}^{\dagger 2}$ for 2-dimensional SCSs. Extending SCSs to multi-dimensional cases would be consistent with employing the same measure to show the performance of amplified states. However, we do not adopt the equivalent-input-noise (EIN) [75] as a measure of noiseless amplification because the expectation value of a quadrature operator, $\langle x_\lambda \rangle$, is zero for all λ for hybrid states and SCSs.

Consequently, we show that the photon addition and subtraction scheme gives higher fidelity while the $(\hat{a}^\dagger)^2$ scheme gives higher gain. Performance of optimal quantum phase estimation measured by quantum Fisher information shows that photon addition and then subtraction scheme is better for relatively small amplitude, where its exact value differs by quantum states, $(\hat{a}^\dagger)^2$ scheme is better for larger amplitude, and the difference of their performance vanishes as amplitude increases.

In Sec. II, we begin with preliminaries of HESs and SCSs. In Sec. III, we investigate and compare the two amplification schemes applied to hybrid states, and in Sec. IV, we investigate and compare those schemes applied to SCSs. In Sec. V, we conclude our paper with assessments of the two amplification schemes.

II. PRELIMINARY

A. Hybrid entangled states

Hybrid entangled states(HES) are bosonic states consisting of entanglement between CV states and DV states. we define a qubit basis of HESs here as

$$\begin{aligned} |\mathcal{H}_\alpha^0\rangle &= \frac{1}{\sqrt{2}}(|0, \alpha\rangle + |1, -\alpha\rangle), \\ |\mathcal{H}_\alpha^1\rangle &= \frac{1}{\sqrt{2}}(|0, \alpha\rangle - |1, -\alpha\rangle), \end{aligned} \quad (1)$$

where $|n, \alpha\rangle = |n\rangle \otimes |\alpha\rangle$, a product of a number state with photon number n and a coherent state with amplitude $\alpha (\in \mathbb{R}^+$ for convenience). For a 2D HES system, The DV part can also be polarization states $|H\rangle$ and $|V\rangle$. Although coherent states $|\pm\alpha\rangle$ are not orthogonal to each other, orthogonality of number states provides independence of normalization factor with respect to amplitude α .

HES qubits can be generalized to represent qudits using d -fold complex roots of 1, $\omega_d := e^{\frac{2\pi i}{d}}$.

$$|\mathcal{H}_{\alpha,d}^k\rangle := \frac{1}{\sqrt{d}} \sum_{n=0}^{d-1} \omega_d^{-kn} |n, \alpha\omega_d^n\rangle, \quad (2)$$

Here k represents the index for the d -dimensional qudit. Overlap between arbitrary basis states can be calculated as

$$\begin{aligned} \langle \mathcal{H}_{\alpha,d}^k | \mathcal{H}_{\alpha,d}^l \rangle &= \frac{1}{d} \sum_{m,n} \omega_d^{km} \omega_d^{-ln} \langle m, \alpha\omega_d^m | n, \alpha\omega_d^n \rangle \\ &= \frac{1}{d} \sum_n \omega_d^{(k-l)n} = \delta_{k,l}. \end{aligned} \quad (3)$$

which indeed shows orthonormality. Also, the photon number statistics of HES are the same with coherent states with the same amplitude. We do not explicitly prove this since the statement can be directly derived from Proposition 1 in Sec. III.

Another important feature of the HES qudits is that photon addition/subtraction maps them to other HES qudits. For a d -dimensional hybrid state $|\mathcal{H}_{\alpha,d}^k\rangle$, m (\hat{a}^\dagger)² maps $|\mathcal{H}_{\alpha,d}^k\rangle$ to $|\mathcal{H}_{\beta,d}^l\rangle$ for some different amplitude β where $l \equiv k + m \pmod{d}$.

$$\begin{aligned} \frac{1}{\mathcal{N}} \langle \mathcal{H}_{\beta,d}^l | (I \otimes (\hat{a}^\dagger)^m) | \mathcal{H}_{\alpha,d}^k \rangle &= \frac{1}{\mathcal{N}d} \sum_n \omega_d^{(l-k)n} \langle \beta\omega_d^n | (\hat{a}^\dagger)^m | \alpha\omega_d^n \rangle = \frac{\beta^m}{\mathcal{N}} \text{Exp}[-\frac{1}{2}(\alpha - \beta)^2] \sum_n \frac{1}{d} \omega_d^{(l-k-m)n} \\ &= \frac{1}{\mathcal{N}} \delta_{l,k+m;d} \beta^m \text{Exp}[-\frac{1}{2}(\alpha - \beta)^2]. \end{aligned} \quad (4)$$

where $\delta_{m,k;d} := \delta_{m,k+d \cdot j}$ with $j \in \mathbb{Z}$. That is, $\delta_{m,k;d} = 1$ if and only if $m \equiv k \pmod{d}$. Also, $\mathcal{N} = \mathcal{N}(\alpha) = \sqrt{\sum_{k=0}^n \frac{(n!)^2}{k!(n-k)!^2} \alpha^{2(n-k)}}$ is a normalization factor from photon additions. The normalization factor $\mathcal{N} \approx \alpha^n$ in the asymptotic limit of $\alpha \gg 1$. In such a limit the optimal choice of β yielding maximal overlap becomes α , and in that case, fidelity is strictly 1. Even if we consider a more realistic regime with smaller amplitudes ($\alpha < 9$), we can achieve $F > 0.99$ with well-chosen β up to ≈ 12 successive photon addition.

Successive photon subtraction acts more trivially to HES qudits than the photon addition. m successive photon subtraction exactly maps $|\mathcal{H}_{\alpha,d}^k\rangle$ to $|\mathcal{H}_{\alpha,d}^{l'}\rangle$ with $l' \equiv k - m \pmod{d}$. Note that we always observe the exact transition to target HES qudit without any assumption or change of amplitude.

B. Superposition of coherent states

Superposition of coherent states(SCS), as the name suggests, is a linear combination of classical coherent states with distinct phases. Typical SCS qubit basis, also known as even/odd cat states are given by

$$\begin{aligned} |\mathcal{C}_\alpha^0\rangle &= \frac{1}{\sqrt{2(1 + e^{-2\alpha^2})}} (|\alpha\rangle + |-\alpha\rangle), \\ |\mathcal{C}_\alpha^1\rangle &= \frac{1}{\sqrt{2(1 - e^{-2\alpha^2})}} (|\alpha\rangle - |-\alpha\rangle). \end{aligned} \quad (5)$$

It is worth noting that individual coherent components are not orthogonal, making the normalization factor of SCS depend on the coherent state amplitude α . Moreover, orthogonality between $|\mathcal{C}_\alpha^0\rangle$ and $|\mathcal{C}_\alpha^1\rangle$ is strictly guaranteed by relative phase between their components regardless of their nonorthogonality. This can be explicitly proven by attaining the number basis expansion of

2D SCSs.

$$\begin{aligned}\langle n | \mathcal{C}_\alpha^0 \rangle &= \frac{1}{\sqrt{2(1 - e^{-2\alpha^2})n!}} (\alpha^n + (-\alpha)^n), \\ \langle n | \mathcal{C}_\alpha^1 \rangle &= \frac{1}{\sqrt{2(1 - e^{-2\alpha^2})n!}} (\alpha^n - (-\alpha)^n).\end{aligned}\quad (6)$$

Since $|\mathcal{C}_\alpha^0\rangle$ only contains number states with even photon number while $|\mathcal{C}_\alpha^1\rangle$ only contains the rest, they are orthogonal.

Generalized d-dimensional SCSs representing qudit basis can be obtained in the same way as the HES case.

$$|\mathcal{C}_{\alpha,d}^k\rangle := N_{k,\alpha,d} \sum_{n=0}^{d-1} \omega_d^{-kn} |\alpha\omega_d^n\rangle, \quad (7)$$

with qudit index k and normalization factor $N_{k,\alpha,d}$ given by

$$N_{k,\alpha,d} = \frac{1}{\sqrt{d \sum_n \omega_d^{-kn} \text{Exp}[-\alpha^2(1 - \omega_d^n)]}}. \quad (8)$$

Orthonormality is again guaranteed by the relative phase of each component canceling all the nonzero overlap of CV parts.

$$\begin{aligned}\langle m | \mathcal{C}_{\alpha,d}^k \rangle &= N_{k,\alpha,d} \sum_n \omega_d^{-kn} \langle m | \alpha\omega_d^n \rangle \\ &= N_{k,\alpha,d} \sum_n \omega_d^{-kn} \frac{(\alpha\omega_d^n)^m}{\sqrt{m!}} \\ &= \frac{\alpha^m N_{k,\alpha,d}}{\sqrt{m!}} \sum_n \omega_d^{n(m-k)} = \frac{\alpha^m N_{k,\alpha,d}}{\sqrt{m!}} \delta_{m,k;d}\end{aligned}\quad (9)$$

Therefore, the qudit $|\mathcal{C}_{\alpha,d}^k\rangle$ consists only of states with $k(\text{mod } d)$ photons. For this reason, SCS is also called pseudo-number state [29]. This also reassures the orthogonality of SCS qudits.

III. AMPLIFICATION OF HYBRID STATE

In this section, we compare the two amplification schemes applied to hybrid states. The first is addition-subtraction, namely $\hat{a}\hat{a}^\dagger$ -scheme, while the second comprises successive photon addition, namely $\hat{a}^{\dagger 2}$ -scheme. Deterministic implementation of both schemes is fundamentally forbidden since they are non-unitary. Thus, quantum channels enabling the probabilistic application of those operations are designed to realize those schemes.

The states after application of both schemes on $|\mathcal{H}_{\alpha,d}^k\rangle$ can be formally written as follows.

$$\begin{aligned}|\mathcal{H}_{\alpha,d}^{k,\hat{a}\hat{a}^\dagger}\rangle &= N_{hyb}^{\hat{a}\hat{a}^\dagger}(\alpha, d) (I \otimes \hat{a}\hat{a}^\dagger) \frac{1}{\sqrt{d}} \sum_n \omega_d^{-kn} |n, \alpha\omega_d^n\rangle \\ |\mathcal{H}_{\alpha,d}^{k,(\hat{a}^\dagger)^2}\rangle &= N_{hyb}^{\hat{a}^{\dagger 2}}(\alpha, d) (I \otimes (\hat{a}^\dagger)^2) \frac{1}{\sqrt{d}} \sum_n \omega_d^{-kn} |n, \alpha\omega_d^n\rangle\end{aligned}\quad (10)$$

where $N_{hyb}^{\hat{a}\hat{a}^\dagger}(\alpha, d)$, $N_{hyb}^{(\hat{a}^\dagger)^2}(\alpha, d)$ normalization factors required for the consequent states to be normalized. Note that we only operate on CV parts.

$$N_{hyb}^{\hat{a},\hat{a}^\dagger}(\alpha, d) = \frac{1}{\sqrt{\alpha^4 + 3\alpha^2 + 1}} \quad (11)$$

$$N_{hyb}^{\hat{a}^{\dagger 2}}(\alpha, d) = \frac{1}{\sqrt{\alpha^4 + 4\alpha^2 + 2}} \quad (12)$$

One can see that the normalization factors do not depend on the dimension d nor qudit index k . This originates from the distinctive structure of HES where individual components are orthogonal to one another. This property of HES provides a way to simplify the calculation of relevant expectation values to a normal ordering problem of bosonic operators.

Proposition 1 For any bosonic operator polynomial $P(\hat{a}, \hat{a}^\dagger)$ with equal degrees of \hat{a} and \hat{a}^\dagger in every term, its expectation value to a HES $|\mathcal{H}_{\alpha,d}^k\rangle$ is same as the expectation value evaluated with a coherent state having same amplitude:

$$\langle P(\hat{a}, \hat{a}^\dagger) \rangle_{\mathcal{H}_{\alpha,d}^k} = \langle P(\hat{a}, \hat{a}^\dagger) \rangle_\alpha \quad (13)$$

Trace preserving property of quantum channels and Proposition 1 gives an expression for normalization factor $N_{hyb}^{P(\hat{a},\hat{a}^\dagger)}(\alpha, d)$:

$$N_{hyb}^{P(\hat{a},\hat{a}^\dagger)}(\alpha, d) = \frac{1}{\sqrt{\langle \alpha | P(\hat{a}, \hat{a}^\dagger)^\dagger P(\hat{a}, \hat{a}^\dagger) | \alpha \rangle}}, \quad (14)$$

which is independent of dimension d and qudit number k as we observed.

we take fidelity and gain as our figures of merit to compare the two schemes ($\hat{a}\hat{a}^\dagger$, $(\hat{a}^\dagger)^2$). Fidelity can be considered as a measure of how close we can get to our target state, while gain quantifies our capability to increase the amplitude of the component states. Let us denote the amplitude of the target state as $g\alpha$ where g is the gain value. For the photon addition and then subtraction scheme, the fidelity is analytically obtained as

$$F^{\hat{a}\hat{a}^\dagger} = \frac{g^2\alpha^4 + 2g\alpha^2 + 1}{\alpha^4 + 3\alpha^2 + 1} \text{Exp}[-\alpha^2(g-1)^2], \quad (15)$$

while for the $(\hat{a}^\dagger)^2$ scheme, the fidelity is obtained as

$$F^{\hat{a}^{\dagger 2}} = \frac{g^4\alpha^4}{\alpha^4 + 4\alpha^2 + 2} \text{Exp}[-\alpha^2(g-1)^2]. \quad (16)$$

The fidelity graphs of the two schemes are shown in Figure 1. (a). One can see that the $\hat{a}\hat{a}^\dagger$ scheme yields higher fidelity than $(\hat{a}^\dagger)^2$ scheme. We first note that the fidelity in Eq. (15) and Eq. (16) are the same for the fidelity of coherent states due to Proposition 1. Explicit calculation of fidelities in Appendix A indeed has the form of Eq. (12). The behavior of fidelity between the

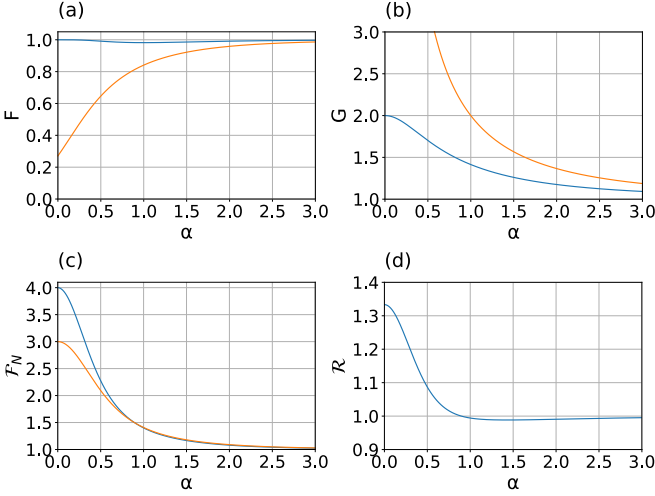


Figure 1: (a) Fidelity graphs of the two schemes, $\hat{a}\hat{a}^\dagger$ and $\hat{a}^{\dagger 2}$. Blue line denotes $F_{hyb}^{\hat{a}\hat{a}^\dagger}$ while orange line denotes $F_{hyb}^{\hat{a}^{\dagger 2}}$. (b) Gain graphs of the two schemes. Blue line denotes $G_{hyb}^{\hat{a}\hat{a}^\dagger}$ while orange line denotes $G_{hyb}^{\hat{a}^{\dagger 2}}$. (c) Ratio of quantum Fisher information of amplified states over those of hybrid states, \mathcal{F}_N . Blue line denotes $\mathcal{F}_{hyb}^{\hat{a}\hat{a}^\dagger}/\mathcal{F}_{hyb}$ while orange line denotes $\mathcal{F}_{hyb}^{\hat{a}^{\dagger 2}}/\mathcal{F}_{hyb}$. (d) Ratio of quantum Fisher information of the two schemes, $\mathcal{R} = \mathcal{F}_{hyb}^{\hat{a}\hat{a}^\dagger}/\mathcal{F}_{hyb}^{\hat{a}^{\dagger 2}}$.

target coherent state with greater amplitude and the coherent state amplified with either $\hat{a}\hat{a}^\dagger$ scheme or $(\hat{a}^\dagger)^2$ scheme are well known [65].

We can generalize this agreement between coherent states and HES qudits. Let us consider a general amplification scheme that employs successive photon addition and subtraction, which can be written as $\hat{a}^{n_1}\hat{a}^{\dagger m_1}\hat{a}^{n_2}\hat{a}^{\dagger m_2}\dots$. We assume that $\sum_i(m_i - n_i) = l$, then it approximately maps $|\mathcal{H}_{\alpha,d}^k\rangle$ to $|\mathcal{H}_{\beta,d}^{k+l}\rangle$ for some β . The normal ordered form of this amplification would be the form of $\sum_i C_i \hat{a}^{\dagger i} \hat{a}^{\dagger l} \hat{a}^i = \hat{a}^{\dagger l} : g(\hat{a}, \hat{a}^\dagger) :$ with every term in $g(\hat{a}, \hat{a}^\dagger)$ containing the same number of creation/annihilation operators, thus an overlap between the amplified state and the target state is written as

$$\begin{aligned} & \langle \mathcal{H}_{\beta,d}^{k+l} | \hat{a}^{\dagger l} : g(\hat{a}, \hat{a}^\dagger) : | \mathcal{H}_{\alpha,d}^k \rangle \\ &= \frac{1}{d} \sum_{m,n} \langle m, \beta \omega^m | (I \otimes \hat{a}^{\dagger l} : g(\hat{a}, \hat{a}^\dagger) :) | n, \alpha \omega^n \rangle \omega^{l(m-n)} \\ &= \frac{1}{d} \sum_n \beta^l \langle \beta \omega^n | : g(\hat{a}, \hat{a}^\dagger) : | \alpha \omega^n \rangle = \beta^l \langle \beta | : g(\hat{a}, \hat{a}^\dagger) : | \alpha \rangle, \end{aligned} \quad (17)$$

which is exactly that of coherent states. That is, we can generalize Proposition 1 further:

Proposition 2 For any bosonic operator polynomial $Q(\hat{a}, \hat{a}^\dagger; l)$ with every term in it satisfying $\deg(\hat{a}) -$

$\deg(\hat{a}^\dagger) = l$,

$$\langle \mathcal{H}_{\beta,d}^{k+l} | Q(\hat{a}, \hat{a}^\dagger; l) | \mathcal{H}_{\alpha,d}^k \rangle = \langle \beta | Q(\hat{a}, \hat{a}^\dagger; l) | \alpha \rangle \quad (18)$$

Unlike Proposition 1, this agreement between fidelity of hybrid state amplification and coherent state amplification does not solely originate from the orthogonality of discrete variables. We both need discrete variables $|n\rangle$ which act as labels of continuous variables $|\alpha \omega_d^n\rangle$ and equal phase factor ω which constitutes both qudit number k by relative phase ω^{-kn} and phase of coherent states $|\alpha \omega^m\rangle$ to cancel out relative phase.

Now let us obtain the gain value defined as the ratio between the amplitudes of the target state to the initial state giving the maximum fidelity. This can be obtained by solving the following equation

$$\frac{dF}{dg} = 0. \quad (19)$$

For the $\hat{a}\hat{a}^\dagger$ scheme, solving the equation gives the gain as

$$g = \frac{\alpha^2 - 1 + \sqrt{\alpha^4 + 6\alpha^2 + 1}}{2\alpha^2}, \quad (20)$$

while for the $(\hat{a}^\dagger)^2$ scheme, solving the equation gives the gain as

$$g = \frac{1 + \sqrt{1 + \frac{8}{\alpha^2}}}{2}. \quad (21)$$

The gain graphs of the two schemes are shown in Fig 1. (b). One can see that the $(\hat{a}^\dagger)^2$ scheme yields higher gain than the $\hat{a}\hat{a}^\dagger$ scheme, converse to the fidelity graphs. The behavior of optimal gain of hybrid state amplification is also identical to that of coherent state amplification for the same reason as fidelity.

We further note that the gain can be defined by the ratio of the expectation values of quadrature operators with an arbitrary phase ϕ [64, 65]. This gain value, however, can be somewhat inadequate for hybrid states because the expectation value of quadrature value with any phase ϕ is zero for hybrid states, as one can confirm with the following equation.

$$\begin{aligned} & \frac{1}{d} \sum_{m,n} \langle m, \alpha \omega^m | I \otimes (\hat{a}e^{i\lambda} + \hat{a}^\dagger e^{-i\lambda}) | n, \alpha \omega^n \rangle \\ &= \frac{1}{d} \sum_n \alpha (e^{i\lambda} \omega^n + e^{-i\lambda} \omega^{-n}) = 0. \end{aligned} \quad (22)$$

Interestingly, however, the ratio is finite and equals that of coherent states. For an arbitrary amplification scheme via photon addition or subtraction, $f(\hat{a}, \hat{a}^\dagger)$, the gain of coherent states defined by the ratio is

$$g = \frac{(N^{f(\hat{a}, \hat{a}^\dagger)})^2 \langle \alpha | f(\hat{a}, \hat{a}^\dagger)^\dagger (\hat{a}e^{i\lambda} + \hat{a}^\dagger e^{-i\lambda}) f(\hat{a}, \hat{a}^\dagger) | \alpha \rangle}{\langle \alpha | (\hat{a}e^{i\lambda} + \hat{a}^\dagger e^{-i\lambda}) | \alpha \rangle}$$

Let us write the normal ordered form of $f(\hat{a}, \hat{a}^\dagger)^\dagger \hat{a} f(\hat{a}, \hat{a}^\dagger)$ as $\sum_i C_i \hat{a}^{\dagger i} \hat{a}^i \hat{a} = g(\hat{a}, \hat{a}^\dagger) \hat{a}$, then the gain is written as

$$g = (N^{f(\hat{a}, \hat{a}^\dagger)})^2 \langle \alpha | g(\hat{a}, \hat{a}^\dagger) | \alpha \rangle \quad (23)$$

Likewise, the gain of hybrid states defined by the ratio is

$$g_{hyb} = (N_{hyb}^{f(\hat{a}, \hat{a}^\dagger)})^2 \langle \alpha | g(\hat{a}, \hat{a}^\dagger) | \alpha \rangle$$

We can go further with this gain to define equivalent input noise (EIN), a measure of noiseless amplification. However, since the expectation value of quadrature is zero, it lacks physical meaning, thus we will not stick to it.

Observing the results so far, $\hat{a}\hat{a}^\dagger$ scheme has an advantage over higher fidelity while $(\hat{a}^\dagger)^2$ has an advantage over higher gain, for all amplitude α . This property gives us a guide on which amplification scheme to use. However, their advantages over different aspects make it hard to compare their overall performance. Qualitatively, we know that $\hat{a}\hat{a}^\dagger$ scheme would be better for small amplitude since coherent states with small amplitude are susceptible to the change of their photon number. Meanwhile, we can guess that the two schemes will not differ so much for large amplitude because coherent states with sufficiently large amplitude are robust against several photon addition or subtraction. Lastly, as a consequence, we can deduce that the $(\hat{a}^\dagger)^2$ scheme would be appropriate for the intermediate amplitude region.

Previous research [65] employed two measures, EIN for coherent states and quantum Fisher information for 2-dimensional SCSs to quantify overall performance which reflects aforementioned qualitative arguments. EIN is a measure of undesired noise generated in the amplification process, thus it is appropriate to measure overall performance. However, we have concluded that EIN lacks physical meaning in our case since the expectation values of quadrature operators are always zero. As an alternative, we take quantum Fisher information for phase estimation as a figure of merit of amplified states, which is defined by

$$\mathcal{F}[\rho, \hat{H}] = 2 \sum_{k,l} \frac{(\lambda_k - \lambda_l)^2}{(\lambda_k + \lambda_l)} |\langle k | \hat{H} | l \rangle|^2, \quad (24)$$

where ρ is a density matrix, $|k\rangle$ is a k -th eigenvector and λ_k is a k -th eigenvalue of the density matrix ρ , \hat{H} is the Hamiltonian operator of the harmonic oscillator. Quantum Fisher information is in direct relationship with the performance of phase estimation, known as the quantum Cramér-Rao bound.

$$\text{var}(\hat{\theta}) \geq \frac{1}{\mathcal{F}(\hat{\theta})} \quad (25)$$

If the state of interest is pure, the quantum Fisher information is easily given by $4\langle \Delta \hat{H} \rangle$, which is proportional

to $4\langle \Delta \hat{n} \rangle$ for optical systems, where \hat{n} is the number operator $\hat{a}^\dagger \hat{a}$. For simplicity, we will call $4\langle \Delta \hat{n} \rangle$ as quantum Fisher information from now on. To begin with, quantum Fisher information of HESs is

$$\mathcal{F}_{hyb} = 4\alpha^2, \quad (26)$$

which is again the same as the coherent state due to Proposition 1. In the same argument of Ref. [65], this supports that quantum Fisher information is a good measure of the overall performance of amplification schemes because both amplitude gain and noiseless property imply larger quantum Fisher information. Also, quantum Fisher information of $\hat{a}\hat{a}^\dagger$ -amplified hybrid states is given by

$$\mathcal{F}_{hyb}^{\hat{a}\hat{a}^\dagger} = \frac{4\alpha^2(\alpha^8 + 6\alpha^6 + 14\alpha^4 + 10\alpha^2 + 4)}{(\alpha^4 + 3\alpha^2 + 1)^2}. \quad (27)$$

lastly, quantum Fisher information of $(\hat{a}^\dagger)^2$ -amplified hybrid states is given by

$$\mathcal{F}_{hyb}^{\hat{a}^{\dagger 2}} = \frac{4\alpha^2(\alpha^8 + 8\alpha^6 + 24\alpha^4 + 24\alpha^2 + 12)}{(\alpha^4 + 4\alpha^2 + 2)^2}. \quad (28)$$

The ratios of quantum Fisher information, $\mathcal{F}_{hyb}^{\hat{a}\hat{a}^\dagger} / \mathcal{F}_{hyb}$ and $\mathcal{F}_{hyb}^{\hat{a}^{\dagger 2}} / \mathcal{F}_{hyb}$, are plotted in Fig 1. (c). The value is always larger than 1 which indicates that hybrid states never become worse in terms of quantum Fisher information. In the asymptotic limit, the ratio converges to 1, implying that the amplification scheme is of no use for sufficiently large amplitude.

For a clear comparison of both schemes, we examined the ratio between two schemes $\mathcal{F}_{hyb}^{\hat{a}\hat{a}^\dagger} / \mathcal{F}_{hyb}^{\hat{a}^{\dagger 2}}$, in Fig 1. (d). The figure shows that up to amplitude $\alpha \approx 0.9$, $\hat{a}\hat{a}^\dagger$ scheme has higher quantum Fisher information. The ratio monotonically decreases up to $\alpha \approx 1.43$, starting from 1.33 at $\alpha = 0$, 1.11 at $\alpha = 0.45$, and 1 at $\alpha \approx 0.9$. After $\alpha \approx 0.9$, $(\hat{a}^\dagger)^2$ scheme yields higher quantum Fisher information for the amplified state. For sufficiently large α , the ratio converges to 1 and the difference is negligible. This result confirms our qualitative analysis.

IV. AMPLIFICATION OF SUPERPOSITIONS OF COHERENT STATES

In this section, we compare the two amplification schemes performed on SCSs. After $\hat{a}\hat{a}^\dagger$ scheme and $(\hat{a}^\dagger)^2$ scheme, SCSs are amplified to

$$N_{SCS}^{\hat{a}\hat{a}^\dagger}(\alpha, k, d) \hat{a}\hat{a}^\dagger \sum_n \omega_d^{-kn} |\alpha \omega_d^n\rangle, \quad (29)$$

and

$$N_{SCS}^{\hat{a}^{\dagger 2}}(\alpha, k, d) (\hat{a}^\dagger)^2 \sum_n \omega_d^{-kn} |\alpha \omega_d^n\rangle, \quad (30)$$

respectively, where $N_{SCS}^{\hat{a}\hat{a}^\dagger}(\alpha, k, d)$ and $N_{SCS}^{\hat{a}^{\dagger 2}}(\alpha, k, d)$ are normalization factors

$$N_{SCS}^{\hat{a}\hat{a}^\dagger}(\alpha, k, d) = \frac{1}{\sqrt{d \sum_n \omega_d^{-kn} (\alpha^4 \omega_d^{2n} + 3\alpha^2 \omega_d^n + 1) \text{Exp}[-\alpha^2(1 - \omega_d^n)]}}, \quad (31)$$

$$N_{SCS}^{\hat{a}^{\dagger 2}}(\alpha, k, d) = \frac{1}{\sqrt{d \sum_n \omega_d^{-kn} (\alpha^4 \omega_d^{2n} + 4\alpha^2 \omega_d^n + 2) \text{Exp}[-\alpha^2(1 - \omega_d^n)]}}. \quad (32)$$

One can see that the normalization factors $N_{SCS}^{\hat{a}^{\dagger 2}}(\alpha, k, d)$ and $N_{SCS}^{\hat{a}\hat{a}^\dagger}(\alpha, k, d)$ both depend on the qudit number k and dimension d , unlike hybrid states.

In the same spirit as Sec. III, we first obtain fidelity

and then obtain gain which is defined by the value that maximizes fidelity. Quantum Fisher information will be employed as an example of the overall performance of the two schemes. For each scheme, fidelity is written as

$$F_{SCS}^{\hat{a}\hat{a}^\dagger} = \frac{\{\sum_n (1 + g\alpha^2 \omega_d^n) \omega_d^{-kn} \text{Exp}[g\alpha^2 \omega_d^n]\}^2}{(\sum_n \omega_d^{-kn} (\alpha^4 \omega_d^{2n} + 3\alpha^2 \omega_d^n + 1) \text{Exp}[\alpha^2 \omega_d^n]) (\sum_n \omega_d^{-kn} \text{Exp}[g^2 \alpha^2 \omega_d^n])}, \quad (33)$$

$$F_{SCS}^{\hat{a}^{\dagger 2}} = \frac{g^4 \alpha^4 \{\sum_n \omega_d^{-kn} \text{Exp}[g\alpha^2 \omega_d^n]\}^2}{(\sum_n \omega_d^{-kn} (\alpha^4 \omega_d^{2n} + 4\alpha^2 \omega_d^n + 2) \text{Exp}[\alpha^2 \omega_d^n]) (\sum_n \omega_d^{-(k+2)n} \text{Exp}[g^2 \alpha^2 \omega_d^n])}. \quad (34)$$

Gain values are given by which maximize the fidelity, by solving following equations.

$$\frac{dF_{SCS}^{\hat{a}\hat{a}^\dagger}}{dg} = 0, \quad \frac{dF_{SCS}^{\hat{a}^{\dagger 2}}}{dg} = 0. \quad (35)$$

This cannot be obtained using elementary functions in closed forms, thus we find the numerical solution. Relations between fidelity and gain for both schemes are shown in Fig 2. and Fig 3. for $d = 3, 4, 5$ with every k . In Fig 2., fidelity and gain of the $\hat{a}\hat{a}^\dagger$ amplification are plotted with respect to the amplitude. Overall shapes of the graphs are not much different from those of hybrid states, however, there are two additional features. (i) The larger the qudit number k , the larger the amplitude α where the local minimum appears. (ii) The larger the qudit number k , the larger the local minimum.

Recall that SCSs with qudit number k , $|\mathcal{C}_{\alpha,d}^k\rangle$, contains $k \pmod{d}$ number of photons. For small amplitude, $\alpha \approx 0$, the coefficient of Fock basis $|n\rangle$ is concentrated on the Fock state with the least number, $|k\rangle$. This explains high fidelity for very low amplitude because the amplification $\hat{a}\hat{a}^\dagger$ does not change the number state, as one can confirm with the following equality

$$\hat{a}\hat{a}^\dagger |k\rangle = (k+1) |k\rangle. \quad (36)$$

As α increases, the SCSs no longer stay in the number state k . $|\mathcal{C}_{\alpha,d}^k\rangle$ contains more and more $|d+k\rangle, |2d+k\rangle, \dots$, Fock states. Then, the additional factor arising from

the amplification becomes relevant and changes the state.

$$\hat{a}\hat{a}^\dagger (|k\rangle + |d+k\rangle) = (k+1) |k\rangle + (d+k+1) |d+k\rangle \\ \not\propto (|k\rangle + |d+k\rangle). \quad (37)$$

This explains the emergence of troughs as α increases. If amplitude α is sufficiently large, every $|\alpha \omega_d^n\rangle$ is orthogonal to each other as one can see from the equation

$$\langle \alpha \omega_d^m | \alpha \omega_d^n \rangle = \text{Exp}[-\alpha^2(1 - \omega_d^{(n-m)})] \longrightarrow \delta_{m,n}, \quad (38)$$

as $\alpha \rightarrow \infty$. Accordingly, the normalization factor $N_{k,\alpha,d}$ converges to $\frac{1}{\sqrt{d}}$ as α grows, thus the difference between the SCSs and hybrid states vanishes. This explains the recovery of high fidelity for large amplitude.

We revisit the pseudo-number property of SCSs to further investigate the behavior of their fidelities against amplified counterparts. First observe from Eq. (9) that as the amplitude α increases, the mean photon number of SCSs grows. While the physical interpretation of the amplitude α renders this intuitive, one can verify it by examining the sign of the derivative. As we mentioned earlier, $|\mathcal{C}_{\alpha,d}^k\rangle$ starts from the Fock state $|k\rangle$ for $\alpha \sim 0$, and obtain coefficients of other Fock states $|d+k\rangle, |2d+k\rangle, \dots$, as α increases. For small qudit-number k , coefficients of other Fock states can be sufficiently large to reduce the fidelity with small amplitude α . This explains why trough appears earlier with smaller qudit-number k . As amplitude α grows, overlap between $\{|\alpha \omega_d^n\rangle\}_n$ becomes smaller, thus recovered orthogonality contributes

to fidelity which makes the depth of trough with larger k shallower than that of smaller k .

With this qualitative analysis, we can predict two additional features that were not seen in Fig 2. First, since the overlap between $\{|\alpha\omega_d^n\rangle\}_n$ increases with d , we need larger amplitude α to recover orthogonality. Then the coefficients of $|2d+k\rangle, |3d+k\rangle, \dots$, can be significantly large before we recover orthogonality, thus it makes multiple troughs, as we showed in Fig 3. Second, for fixed k , there is no monotonic tendency of the depth of troughs concerning d because two factors antagonize each other. If d grows, overlap between $\{|\alpha\omega_d^n\rangle\}_n$ increases, but the required amplitude α to see trough becomes large, contributing to orthogonality. One can see that the depth of troughs of qudit number 0 with $d=3$ is deeper than that of $d=2$ and $d=4$.

The gain graphs do not show any particular behavior. As α increases, more and more photons SCSs have, thus contribution to the gain of $\hat{a}\hat{a}^\dagger$ scheme monotonically decreases with α .

In Fig 3., we plot fidelities and gains against the state amplitude α in the $(\hat{a}^\dagger)^2$ case. The most noticeable feature is that only two states show different behavior for fidelity and gain. we focus on the fact that the qudit-number of two states are the last two, that is, $d-2$ and $d-1$ to explain the behavior of the two states. Recall that a qudit number k is mapped to $k+2 \pmod d$

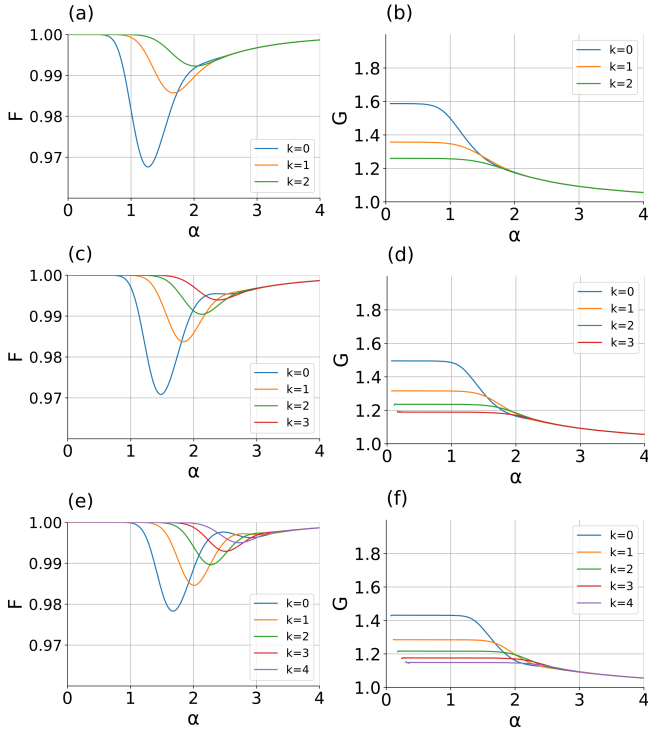


Figure 2: For SCSs, $\hat{a}\hat{a}^\dagger$ scheme, (a) Fidelity plot of $d=3$. (b) Optimal gain plot of $d=3$. (c) Fidelity plot of $d=4$. (d) Optimal plot of $d=4$. (e) Fidelity plot of $d=5$. (f) Optimal gain plot of $d=5$.

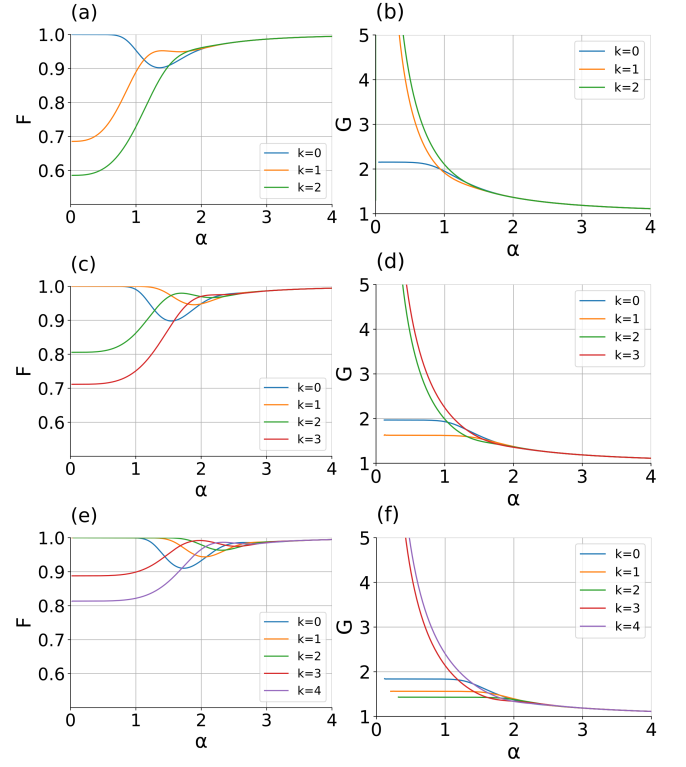


Figure 3: For SCSs, $\hat{a}^{\dagger 2}$ scheme, (a) Fidelity graphs of $d=3$. (b) Gain graphs of $d=3$. (c) Fidelity graphs of $d=4$. (d) Gain graphs of $d=4$. (e) Fidelity graphs of $d=5$. (f) Gain graphs of $d=5$.

via $(\hat{a}^\dagger)^2$ amplification, thus our target states are $|\mathcal{C}_{\beta,d}^0\rangle$ and $|\mathcal{C}_{\beta,d}^1\rangle$. For sufficiently large α , it does not make any special behavior due to orthogonality. However, for small amplitude, $\alpha \sim 0$, since $|\mathcal{C}_{\alpha,d}^{(d-2)}\rangle \sim |d-2\rangle$ and $|\mathcal{C}_{\alpha,d}^{(d-1)}\rangle \sim |d-1\rangle$, the $(\hat{a}^\dagger)^2$ scheme maps most of their coefficients to $|d\rangle$ and $|d+1\rangle$, which do not have large overlap with $|\mathcal{C}_{\alpha,d}^0\rangle \sim |0\rangle$ and $|\mathcal{C}_{\alpha,d}^1\rangle \sim |1\rangle$. This makes low fidelity for the states with qudit-number $d-2$ and $d-1$. Moreover, the target states should have large amplitude α to have coefficients of $|d\rangle$ and $|d+1\rangle$, thus the ratio between the amplitude of the target state and that of the initial state diverges, which explains the behavior of the gain graphs for small α . As α increases, target states have larger coefficients of $|d\rangle, |2d\rangle, \dots$ and $|d+1\rangle, |2d+1\rangle, \dots$, thus their fidelity increase and gain values decrease. Furthermore, for small amplitude α , with the same reason of troughs appears in $\hat{a}\hat{a}^\dagger$ amplification, fidelity is higher for $|\mathcal{C}_{\alpha,d}^{(d-2)}\rangle$, and thus the gain is higher for $|\mathcal{C}_{\alpha,d}^{(d-1)}\rangle$. As α increases, they can be reversed as one can see in Fig 3., (e) and (f) with $\alpha \approx 2.2$. Other states except for the last two show similar behavior to Fig 2. Their troughs are deeper than those of $\hat{a}\hat{a}^\dagger$

state because $(\hat{a}^\dagger)^2$ changes photon number more than $\hat{a}\hat{a}^\dagger$. This makes lower fidelity and higher gain, which is also observed for hybrid states or coherent states [65].

Now, we will investigate quantum Fisher information of the SCSs and the amplified SCSs to compare their

performance of optimal phase estimation, as we did in section III. Quantum Fisher information of SCSs and amplified SCSs under $\hat{a}\hat{a}^\dagger$ and $(\hat{a}^\dagger)^2$ schemes are calculated to be

$$\mathcal{F}_{SCS} = 4\alpha^2 \frac{\sum_n (\alpha^2 \omega_d^{(2-k)n} + \omega_d^{(1-k)n}) \text{Exp}[\alpha^2 \omega_d^n]}{\sum_n \omega_d^{-kn} \text{Exp}[\alpha^2 \omega_d^n]} - 4\alpha^4 \left(\frac{\sum_n \omega_d^{(1-k)n} \text{Exp}[\alpha^2 \omega_d^n]}{\sum_n \omega_d^{-kn} \text{Exp}[\alpha^2 \omega_d^n]} \right)^2 \quad (39)$$

$$\mathcal{F}_{SCS}^{\hat{a}\hat{a}^\dagger} = \frac{4 \sum_n (\alpha^8 \omega_d^{4n} + 8\alpha^6 \omega_d^{3n} + 14\alpha^4 \omega_d^{2n} + 4\alpha^2 \omega_d^n) \text{Exp}[\alpha^2 \omega_d^n] \omega_d^{-kn}}{\sum_n (\alpha^4 \omega_d^{2n} + 3\alpha^2 \omega_d^n + 1) \omega_d^{-kn} \text{Exp}[\alpha^2 \omega_d^n]} - 4 \left(\frac{\sum_n (\alpha^6 \omega_d^{3n} + 5\alpha^4 \omega_d^{2n} + 4\alpha^2 \omega_d^n) \text{Exp}[\alpha^2 \omega_d^n] \omega_d^{-kn}}{\sum_n (\alpha^4 \omega_d^{2n} + 3\alpha^2 \omega_d^n + 1) \omega_d^{-kn} \text{Exp}[\alpha^2 \omega_d^n]} \right)^2 \quad (40)$$

$$\mathcal{F}_{SCS}^{\hat{a}^{\dagger 2}} = \frac{4 \sum_n (\alpha^8 \omega_d^{4n} + 13\alpha^6 \omega_d^{3n} + 46\alpha^4 \omega_d^{2n} + 46\alpha^2 \omega_d^n + 8) \text{Exp}[\alpha^2 \omega_d^n] \omega_d^{-kn}}{\sum_n (\alpha^4 \omega_d^{2n} + 4\alpha^2 \omega_d^n + 2) \omega_d^{-kn} \text{Exp}[\alpha^2 \omega_d^n]} - 4 \left(\frac{\sum_n (\alpha^6 \omega_d^{3n} + 8\alpha^4 \omega_d^{2n} + 14\alpha^2 \omega_d^n + 4) \text{Exp}[\alpha^2 \omega_d^n] \omega_d^{-kn}}{\sum_n (\alpha^4 \omega_d^{2n} + 4\alpha^2 \omega_d^n + 2) \omega_d^{-kn} \text{Exp}[\alpha^2 \omega_d^n]} \right)^2 \quad (41)$$

One can see that quantum Fisher information of d -dimensional SCSs is not a monotonic function with respect to amplitude α , thus we cannot follow the argument in Sec. III and Ref. [65] that Fisher information reflects amplification gain and noiseless property. In Fig. 4, we plotted quantum Fisher information of SCSs for $d = 2, 3, 4$ and 5 . For $d = 2$, the graphs smoothly increase with amplitude, and for $d = 3$, the graph shows some fluctuation but still three graphs monotonically increase with amplitude. However, for $d = 4$ and $d = 5$, the fluctuation width becomes so large that they lose monotonic behavior. This shows that quantum Fisher information is not a good measure of the overall performance of noiseless amplification for high dimensions. Smooth and monotonic behavior of quantum Fisher information of SCSs only appears at $d = 2$, even and odd cat states, which were the main interest of Ref. [65]. Therefore, quantum Fisher information for d -dimensional SCSs should be considered as a performance of optimal phase estimation, one of the criteria to compare with other optical states since phase estimation is a popular task in quantum optics, while it is a good measure of overall performance of amplification for hybrid states and $d = 2$ SCSs.

We analyze the fluctuating behavior of quantum Fisher information of SCSs with pseudo-number property. First, observe that Fock states are invariant under phase rotation. This implies that we cannot use the Fock state for phase estimation, which is reflected in quantum Fisher information that $\mathcal{F}_{|n\rangle} = 0$ for any Fock state $|n\rangle$. As we

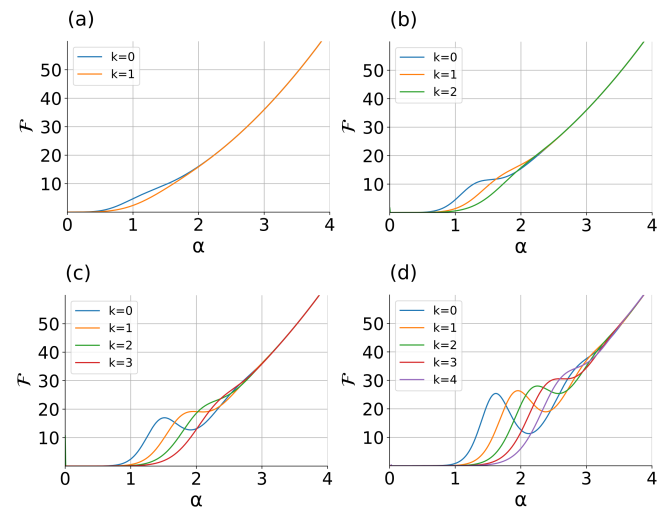


Figure 4: Quantum Fisher information of SCSs for (a) $d=2$, (b) $d=3$, (c) $d=4$ and (d) $d=5$.

investigated, $|\mathcal{C}_{\alpha,d}^k\rangle \sim |k\rangle$ for $\alpha \sim 0$, thus their quantum Fisher information are nearly zero. As amplitude grows, $|\mathcal{C}_{\alpha,d}^k\rangle$ moves to the superposition of Fock states thus its quantum Fisher information increases. As amplitude grows further where $|\mathcal{C}_{\alpha,d}^k\rangle$ begins to concentrate to some Fock state $|d \cdot n + k\rangle$, its quantum Fisher infor-

mation begins to decrease. Further growing amplitude makes $|\mathcal{C}_{\alpha,d}^k\rangle$ be a superposition of Fock states again, thus its quantum Fisher information increases... This explains the fluctuation of quantum Fisher information graphs, and it is the same analysis as that of fidelity graphs. Therefore, in the same reason, it is easily deduced why the width of fluctuation enlarges and the amplitude, where peaks and troughs appear, increases as d grows.

To compare quantum Fisher information of each scheme, we plot graphs of $\mathcal{R} = \mathcal{F}_{SCS}^{\hat{a}\hat{a}^\dagger} / \mathcal{F}_{SCS}^{\hat{a}^{\dagger 2}}$ for $d = 2, 3, 4, 5$ in Fig. 5, as we did for hybrid states. The graph seems to coincide with our earlier qualitative analysis. However, we point out that some regions where $\hat{a}\hat{a}^\dagger$ yields larger quantum Fisher information than that of $\hat{a}^{\dagger 2}$ appear as d increases. For example, for $|\mathcal{C}_{\alpha,5}^0\rangle$, \mathcal{R} is larger than 1 in $1.9 < \alpha < 2.5$ region, where $\mathcal{F}_{SCS}^{\hat{a}^{\dagger 2}}$ is in trough. For sufficiently large amplitude, \mathcal{R} converges to 1, and the two schemes do not show a difference.

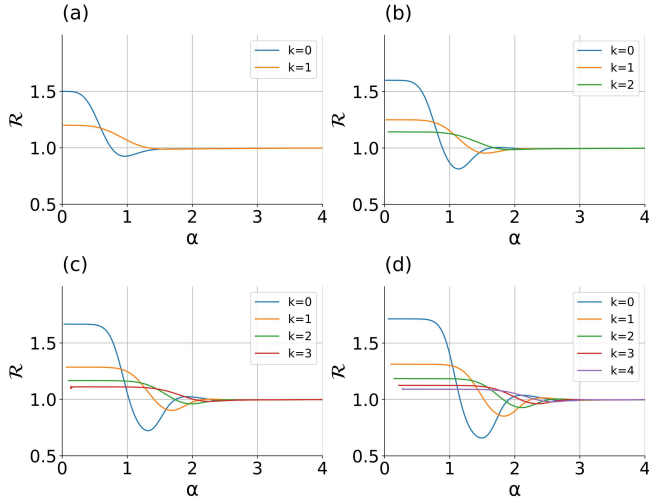


Figure 5: Ratio $\mathcal{R} = \mathcal{F}_{SCS}^{\hat{a}\hat{a}^\dagger} / \mathcal{F}_{SCS}^{\hat{a}^{\dagger 2}}$ for (a) $d=2$, (b) $d=3$, (c) $d=4$, (d) $d=5$.

The graphs of the ratio of quantum Fisher information of amplified SCSs over those of SCSs are plotted in Fig 6., for $d = 3, 4, 5$ with every k . For small amplitude, \mathcal{F}_N of all states under the two schemes are much higher than 1, which means that the performance of amplification for quantum phase estimation is good. After the plateau, the graphs rapidly decrease and fluctuate for SCSs with high d , and reach 1 eventually. Due to the non-monotonic behavior of graphs, an amplification scheme should be chosen considering the goals of the experimentalist and the conditions of SCSs.

V. CONCLUSION

We have investigated two amplification schemes, the photon-addition-and-then-subtraction scheme and the

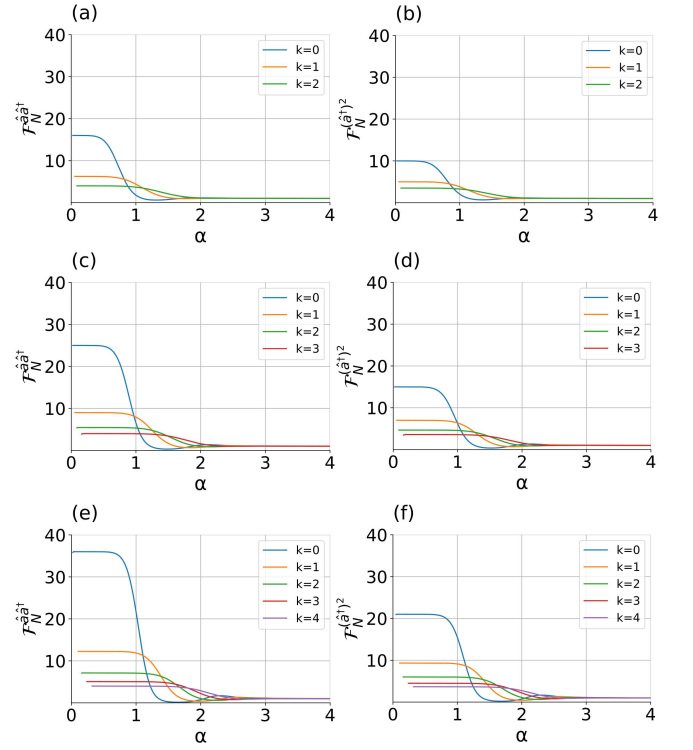


Figure 6: Normalized Fisher information \mathcal{F}_N of SCSs, where (a) $d = 3, \hat{a}\hat{a}^\dagger$, (b) $d = 3, \hat{a}^{\dagger 2}$, (c) $d = 4, \hat{a}\hat{a}^\dagger$, (d) $d = 4, \hat{a}^{\dagger 2}$, (e) $d = 5, \hat{a}\hat{a}^\dagger$, (f) $d = 5, \hat{a}^{\dagger 2}$. Here, \mathcal{F}_N is defined by $\mathcal{F}^{\hat{A}} / \mathcal{F}$, where \hat{A} denotes amplification scheme, $\hat{a}\hat{a}^\dagger$ or $\hat{a}^{\dagger 2}$

$(\hat{a}^\dagger)^2$ scheme, applied to two types of nonclassical states, *i.e.*, hybrid states and SCSs. We have obtained fidelity, gain, and quantum Fisher information of each scheme for each state. For both the schemes, the photon addition and then subtraction scheme has the advantage of higher fidelity, thus it is appropriate for amplifying states with relatively low amplitudes. On the contrary, the $(\hat{a}^\dagger)^2$ scheme has the advantage of higher gain, and it is better for amplifying states with intermediate amplitudes. For sufficiently large amplitudes, the difference between the two schemes vanishes.

For hybrid states, the fidelity and gain under both the schemes are the same as those for the case of coherent states, independent of dimension d or qudit number k due to the orthogonality of the DV part $\{|n\rangle\}_n$. We have obtained quantum Fisher information of hybrid states that reflects the overall performance of the noiseless amplification. Our analysis shows that the photon addition and then subtraction scheme is better for amplitude between 0 and 0.9, and the $(\hat{a}^\dagger)^2$ scheme is better for amplitude larger than 0.9.

For SCSs, behaviors of the fidelity and gain depend on dimension d and qudit number k . In a fidelity graph, a smaller qudit number k shows trough(s) for smaller amplitude with larger depth. In gain graphs, similar behavior is observed but two states with the last two qudit numbers $d - 2$ and $d - 1$ act very differently. We

have analyzed the graph focusing on the pseudo-number property of the superposition of coherent states. Unlike hybrid states, quantum Fisher information graphs show fluctuations as amplitude increases and thus do not reflect the overall performance of noiseless amplification except $d = 2$. Consequently, quantum Fisher information is adopted as an example of the performance of amplified superposition of coherent states, and consistent criterion extended from even and odd cat states, to compare with other optical states. Since fidelity and gain graphs are not trivial, and quantum Fisher information does not indicate overall performance, an appropriate amplification scheme should be chosen considering the goals and con-

ditions of initial states.

ACKNOWLEDGEMENTS

This work was supported by the National Research Foundation of Korea (NRF) grant funded by the Korea government (MSIT) (Nos. RS-2024-00413957, RS-2024-00438415, NRF-2023R1A2C1006115, RS-2024-00437191, and NRF-2022M3K4A1097117) and by the Institute of Information & Communications Technology Planning & Evaluation (IITP) grant funded by the Korea government (MSIT) (IITP-2021-0-01059 and IITP-2023-2020-0-01606).

-
- [1] H. Jeong, A. Zavatta, M. Kang, S.-W Lee, L. S. Constanzo, S. Grandi, T. C. Ralph and M. Bellini, Generation of hybrid entanglement of light, *Nat. Photonics* **8**, 564 (2014).
- [2] O. Morin, K. Juang, J. Liu, H. L. Jeannic, C. Fabre, and J. Laurat, Remote creation of hybrid entanglement between particle-like and wave-like optical qubits, *Nat. Photonics* **8**, 570 (2014).
- [3] B. Yurke and D. Stoler, Generating quantum mechanical superpositions of macroscopically distinguishable states via amplitude dispersion, *Phys. Rev. Lett.* **57**, 13 (1986).
- [4] W. Schleich, M. Pernigo, and F. L. Kien, Nonclassical state from two pseudoclassical states, *Phys. Rev. A* **44**, 2172 (1991).
- [5] H. Jeong, Converting qubits, *Nat. Photonics* **17**(2), 131 (2023)
- [6] A.E. Ulanov, D. Sychev, A.A. Pushkina, I.A. Fedorov, and A.I. Lvovsky, Quantum teleportation between discrete and continuous encodings of an optical qubit, *Phys. Rev. Lett.* **118**, 160501 (2017).
- [7] D.V. Sychev, A.E. Ulanov, E.S. Tiunov, A.A. Pushkina, Entanglement and teleportation between polarization and wave-like encodings of an optical qubit, *Nat. Comm.* **9**, 3672 (2018).
- [8] T. Darras, B. E. Asenbeck, G. Guccione, A. Cavaillés, H. Le Jeannic, and J. Laurat, A quantum-bit encoding converter, *Nat. Photonics*, **17**(2), 165 (2023)
- [9] H. Kwon and H. Jeong, Violation of the Bell-Cluser-Horne-Shimony-Holt inequality using imperfect photodetectors with optical hybrid states, *Phys. Rev. A* **88**, 052127 (2013).
- [10] K. Park, S.-W Lee, and H. Jeong, Quantum teleportation between particlelike and fieldlike qubits using hybrid entanglement under decoherence effects, *Phys. Rev. A* **86**, 062301 (2012).
- [11] H. Jeong, S. Bae, and S. Choi, Quantum teleportation between a single-rail single-photon qubit and a coherent-state qubit using hybrid entanglement under decoherence effects, *Quant. Info. Proc.* **15**, 913 (2016).
- [12] H. Kim, S.-W Lee, and H. Jeong, Two different types of optical hybrid qubits for teleportation in a lossy environment, *Quant. Info. Proc.* **15**, 4729 (2016).
- [13] S.-W Lee, H. Jeong, Near-deterministic quantum teleportation and resource-efficient quantum computation using linear optics and hybrid qubits, *Phys. Rev. A* **87**, 022326 (2013).
- [14] S. Omkar, Y.-S. Teo, and H. Jeong, Resource-efficient topological fault-tolerant quantum computation with hybrid entanglement of light, *Phys. Rev. Lett.* **125**, 060501 (2020).
- [15] Y. Lim, J. Joo, T. P. Spiller, and H. Jeong, Loss-resilient photonic entanglement swapping using optical hybrid states, *Phys. Rev. A* **94**, 062337 (2016).
- [16] S. Bose, J. Singh, A. Cabello, and H. Jeong, Long-distance entanglement sharing using hybrid states of discrete and continuous variables, *Phys. Rev. Applied* **21**, 064103 (2024).
- [17] H. Jeong and M. S. Kim, Purification of entangled coherent states, *Quantum Information and Computation* **2**, 208 (2002).
- [18] A. Cavaillés, H. Le Jeannic, J. Raskop, G. Guccione, D. Markham, E. Diamanti, M. D. Shaw, V. B. Verma, S. W. Nam, and J. Laurat, Demonstration of Einstein-Podolsky-Rosen steering using hybrid continuous-and discrete-variable entanglement of light, *Phys. Rev. Lett.* **121**, 170403 (2018).
- [19] X. Huang, E. Zeuthen, Q. Gong, and Q. He, Engineering asymmetric steady-state Einstein-Podolsky-Rosen steering in macroscopic hybrid systems, *Phys. Rev. A* **100**, 012318 (2019).
- [20] C. Gerry, Generation of optical macroscopic quantum superposition states via state reduction with a Mach-Zehnder interferometer containing a Kerr medium, *Phys. Rev. A* **59**, 4095-4098 (1999).
- [21] K. Nemoto and W. J. Munro, Nearly deterministic linear optical controlled-NOT gate, *Phys. Rev. Lett.* **93**, 250502 (2004).
- [22] H. Jeong, Using weak nonlinearity under decoherence for macroscopic entanglement generation and quantum computation, *Phys. Rev. A* **072** 034305, (2005).
- [23] U. L. Anderson and J. S. Neergaard-Nielsen, Heralded generation of a micro-macro entangled state, *Phys. Rev. A* **88**, 022337 (2013).
- [24] P. T. Cochrane, G. J. Milburn, and W. J. Munro, Macroscopically distinct quantum-superposition states as a bosonic code for amplitude damping, *Phys. Rev. A* **59**, 2631 (1999).

- [25] H. Jeong and M. S. Kim, Efficient quantum computation using coherent states, *Phys. Rev. A* **65**, 042305 (2002).
- [26] T. C. Ralph, A. Gilchrist, G. J. Milburn, W. J. Munro, and S. Glancy, Quantum computation with optical coherent states, *Phys. Rev. A* **68**, 042319 (2003).
- [27] A. P. Lund, T. C. Ralph, and H. L. Haselgrove, Fault-tolerant linear optical quantum computing with small-amplitude coherent states, *Phys. Rev. Lett.* **100**, 030503 (2008).
- [28] C. R. Myers and T. C. Ralph, Coherent state topological cluster state production, *New J. Phys.* **13**, 115015 (2011).
- [29] J. Kim, J. Lee, S.-W Ji, H. Nha, P. M. Anisimov, and J. P. Dowling, Coherent-state optical qudit cluster state generation and teleportation via homodyne detection, *Opt. Comm.* **337**, 79 (2015).
- [30] S. J. van Enk and O. Hirota, Entangled coherent states: Teleportation and decoherence, *Phys. Rev. A* **64**, 022313 (2001).
- [31] H. Jeong, M. S. Kim, and J. Lee, Quantum-information processing for a coherent superposition state via a mixed-entangled coherent channel, *Phys. Rev. A* **64**, 052308(2001).
- [32] J. S. Neergaard-Nielsen, Y. Eto, C.-W. Lee, H. Jeong, and M. Sasaki, Quantum tele-amplification with a continuous-variable superposition state, *Nat. Photonics.* **7**, 439 (2013).
- [33] C. Gerry and R. Campos, Generation of maximally entangled photonic states with a quantum-optical Fredkin gate, *Phys. Rev. A* **64**, 063814 (2001).
- [34] C. Gerry, A. Benmoussa, and R. Campos, Nonlinear interferometer as a resource for maximally entangled photonic states: Application to interferometry, *Phys. Rev. A* **66**, 013804 (2002).
- [35] T. C. Ralph, Coherent superposition states as quantum rulers, *Phys. Rev. A* **65**, 042313 (2002).
- [36] W. J. Munro, K. Nemoto, G. J. Milburn, and S. Braunstein, Weak-force detection with superposed coherent states, *Phys. Rev. A* **66**, 023819 (2002).
- [37] R. Campos, C. Gerry, and A. Benmoussa, Optical interferometry at the Heisenberg limit with twin Fock states and parity measurements, *Phys. Rev. A* **68**, 023810 (2003).
- [38] J. Joo, W. J. Munro, and T. P. Spiller, Quantum metrology with entangled coherent states, *Phys. Rev. Lett.* **107**, 083601 (2011).
- [39] O. Hirota, K. Kato, and D. Murakami, Effectiveness of entangled coherent state in quantum metrology, <http://arxiv.org/abs/1108.1517> (2011).
- [40] J. Joo, K. Park, H. Jeong, W. J. Munro, K. Nemoto, and T. P. Spiller, Quantum metrology for nonlinear phase shifts with entangled coherent states, *Phys. Rev. A* **86**, 043828 (2012).
- [41] Y. M. Zhang, X. W. Li, W. Yang, and G. R. Jin, Quantum Fisher information of entangled coherent states in the presence of photon loss, *Phys. Rev. A* **88**, 043832 (2013).
- [42] H. M. Vasconcelos, L. Sanz, S. Glancy, All-optical generation of states for “Encoding a qubit in an oscillator”, *Opt. Lett.* **35**, 3261–3263 (2010).
- [43] D. J. Weigand, B. M. Terhal, Generating grid states from Schrödinger-cat states without postselection, *Phys. Rev. A* **97**, 022341 (2018).
- [44] S. Konno **et al.**, Logical states for fault-tolerant quantum computation with propagating light, *Science* **383**, 289 (2024).
- [45] L. Li, C.-L. Zou, V. V. Albert, S. Muralidharan, S. M. Girvin and L. Jiang, Cat codes with optimal decoherence suppression for a lossy bosonic channel, *Phys. Rev. Lett.* **119**, 030502 (2017).
- [46] J. Hastrup, U. L. Andersen, All-optical cat-code quantum error correction, *Phys. Rev. Res.* **4**, 043065. (2022).
- [47] D. Wilson, H. Jeong and M. S. Kim, Quantum nonlocality for a mixed entangled coherent state, *J. Mod. Opt.* **49**, 851 (2002).
- [48] C.-Y. Park and H. Jeong, Bell-inequality tests using asymmetric entangled coherent states in asymmetric lossy environments, *Phys. Rev. A* **91**, 042328 (2015).
- [49] M. Paternostro and H. Jeong, Testing non-local realism with entangled coherent states, *Phys. Rev. A* **81**, 032115 (2010).
- [50] C.-W. Lee, M. Paternostro, and H. Jeong, Faithful test of nonlocal realism with entangled coherent states, *Phys. Rev. A* **83**, 022102 (2011).
- [51] J. S. Neergaard-Nielsen, B. M. Nielson, C. Hettich, K. Mølmer, and E. S. Polzik, Generation of a Superposition of Odd Photon Number States for Quantum Information Networks, *Phys. Rev. Lett.* **97**, 083604 (2006).
- [52] A. Ourjoumtsev, H. Jeong, R. Tualle-Brouri and Ph. Grangier, Generation of optical ‘Schrödinger cats’ from photon number states, *Nature.* **448**, 784 (2007).
- [53] K. Wakui, H. Takahashi, A. Furusawa, and M. Sasaki, Photon subtracted squeezed states generated with periodically poled KTiOPO4, *Opt. Express* **15**, 3568 (2007).
- [54] A. Ourjoumtsev, F. Ferreyrol, R. Tualle-Brouri, and P. Grangier, Preparation of non-local superpositions of quasi-classical light states, *Nature Phys.* **5**, 189–192 (2009).
- [55] A. Ourjoumtsev, R. Tualle-Brouri, J. Laurat, and P. Grangier, Generating optical Schrodinger kittens for quantum information processing, *Science* **312**, 83 (2006).
- [56] H. Jeong, A. P. Lund, and T. C. Ralph, Production of superpositions of coherent states in traveling optical fields with inefficient photon detection, *Phys. Rev. A* **72**, 013801 (2005).
- [57] A. P. Lund, H. Jeong, T. C. Ralph, and M. S. Kim, Conditional production of superpositions of coherent states with inefficient photon detection, *Phys. Rev. A* **70**, 020101 (2004).
- [58] D.V. Sychev, A.E. Ulanov, A.A. Pushkina, M.W. Richards, I.A. Fedorov, and A.I. Lvovsky, Enlargement of optical Schrödinger’s cat states, *Nature Photonics* **11**, 379 (2017).
- [59] C. Oh and H. Jeong, Efficient amplification of superpositions of coherent states using input states with different parities, *J. Opt. Soc. Am. B* **35**, 2933 (2018).
- [60] A. Laghaout, J.S. Neergaard-Nielsen, I. Rig3141as, C. Kragh, A. Tipsmark, and U.L. Andersen, Amplification of realistic Schrödinger-cat-state-like states by homodyne heralding, *Phys. Rev. A* **87**, 043826 (2013).
- [61] Y.-B. Sheng, L. Zhou, and G.-L Long, Hybrid entanglement purification for quantum repeaters, *Phys. Rev. A* **88**, 022302 (2013).
- [62] C. Caves, Quantum limits on noise in linear amplifiers, *Phys. Rev. D* **26**, 1817 (1982).
- [63] V. Parigi, A. Zavatta, and M. Bellini, Manipulating thermal light states by the controlled addition and subtraction

tion of single photons, *Laser Phys. Lett.* **5**, 3 (2007).

- [64] A. Zavatta, J. Fiurášek and M. Bellini, A high-fidelity noiseless amplifier for quantum light states, *Nat. Photonics* **5**, 52 (2011).
- [65] J. Park, J. Joo, A. Zavatta, M. Bellini and H. Jeong, Efficient noiseless linear amplification for light fields with larger amplitudes, *Opt. Express* **24**, 1331 (2016).
- [66] C. W. Helstrom, *Mathematics in Science and Engineering* (Academic Press, New York, 1976), Vol. 123.
- [67] S. L. Braunstein and C. M. Caves, Statistical distance and the geometry of quantum states, *Phys. Rev. Lett.* **72**, 3439 (1994).
- [68] O. E. Barndorff-Nielsen, R. D. Gill, Fisher information in quantum statistics, *J. Phys. A* **30**, 4481 (2000).
- [69] M. G. A. Paris, Quantum estimation for quantum technology, *Int. J. Quantum Inf.* **7**, 125 (2009).
- [70] D. Petz, C. Ghinea, Introduction to Quantum Fisher information, In *Quantum Probability and Related Topic*, 261 (2011)
- [71] M. A. Usuga, C. R. Müller, C. Wittmann, P. Marek, R. Filip, C. Marquardt, G. Leuchs, and U. L. Andersen, Noise-powered probabilistic concentration of phase information, *Nat. Phys.* **6**, 767 (2010).
- [72] M. G. Genoni, S. Olivares, and M. G. A. Paris, Optical Phase Estimation in the Presence of Phase Diffusion, *Phys. Rev. Lett.* **106**, 153603 (2011).
- [73] A. A. Berni, T. Gehring, B. M. Nielsen, V. Händchen, M. G. A. Paris, and U. L. Andersen, Ab initio quantum-enhanced optical phase estimation using real-time feedback control, *Nat. Photonics* **9**, 577 (2015).
- [74] S. Izumi, M. Takeoka, K. Wakui, M. Fujiwara, K. Ema, and M. Sasaki, Optical phase estimation via the coherent state and displaced-photon counting, *Phys. Rev. A* **94**, 033842 (2016).
- [75] Ph. Grangier, J.-M. Courty, and S. Reynaud, Characterization of nonideal quantum non-demolition measurements, *Opt. Commun.* **89**, 99 (1992).

VI. APPENDICES

A. Appendix A

The fidelity, gain, and quantum Fisher information of hybrid states are calculated here. The fidelity between the target state and the amplified d -dimensional hybrid states under the photon addition and then subtraction scheme is

$$\begin{aligned} F^{\hat{a}\hat{a}^\dagger} &= N_{hyb}^{\hat{a}\hat{a}^\dagger}(\alpha, d)^2 \left| \frac{1}{d} \sum_{n,m} \langle n, g\alpha\omega_d^n | \hat{a}\hat{a}^\dagger | m, \alpha\omega_d^m \rangle \right|^2 \\ &= \frac{|\sum_n \langle g\alpha\omega_d^n | (1 + \hat{a}^\dagger\hat{a}) | \alpha\omega_d^n \rangle|^2}{d^2(\alpha^4 + 3\alpha^2 + 1)} \\ &= \frac{g^2\alpha^4 + 2g\alpha^2 + 1}{\alpha^4 + 3\alpha^2 + 1} \text{Exp}[-\alpha^2(g-1)^2]. \end{aligned} \quad (42)$$

The fidelity between the target state and the amplified state for d -dimensional hybrid states under the $(\hat{a}^\dagger)^2$

scheme is

$$\begin{aligned} F^{\hat{a}^{\dagger 2}} &= N_{hyb}^{\hat{a}^{\dagger 2}}(\alpha, d)^2 \left| \frac{1}{d} \sum_{n,m} \omega_d^{2n} \langle n, g\alpha\omega_d^n | \hat{a}^{\dagger 2} | m, \alpha\omega_d^m \rangle \right|^2 \\ &= \frac{|\sum_n \omega_d^{2n} \langle g\alpha\omega_d^n | (\hat{a}^{\dagger 2}) | \alpha\omega_d^n \rangle|^2}{d^2(\alpha^4 + 4\alpha^2 + 2)} \\ &= \frac{g^4\alpha^4}{(\alpha^4 + 4\alpha^2 + 2)} \text{Exp}[-\alpha^2(g-1)^2]. \end{aligned} \quad (43)$$

Gain values that maximize the fidelity are obtained by solving the Eq. (19). For photon addition and then subtraction, the equation reduces to

$$(g\alpha^2 + 1)\{1 - (g\alpha^2 + 1)(g-1)\} = 0. \quad (44)$$

Since g and α are positive, we have

$$1 - (g\alpha^2 + 1)(g-1) = 0, \quad (45)$$

which gives

$$g = \frac{\alpha^2 - 1 + \sqrt{\alpha^4 + 6\alpha^2 + 1}}{2\alpha^2}. \quad (46)$$

For $(\hat{a}^\dagger)^2$ scheme, the Eq. (19) reduces to

$$g^2 - g - \frac{2}{\alpha^2} = 0, \quad (47)$$

which gives

$$g = \frac{1 + \sqrt{1 + \frac{8}{\alpha^2}}}{2}. \quad (48)$$

Quantum Fisher information of a pure state is given by $4\langle\Delta\hat{H}\rangle$ which is proportional to $4\langle\Delta\hat{n}\rangle$ for optics system. Using creation operators and annihilation operators and their relation $[\hat{a}, \hat{a}^\dagger] = 1$, we will compute $4\langle\hat{a}^{\dagger 2}\hat{a}^2\rangle + 4\langle\hat{a}^\dagger\hat{a}\rangle - 4\langle\hat{a}^\dagger\hat{a}\rangle^2$. Quantum Fisher information of bare hybrid states is calculated as

$$\begin{aligned} \mathcal{F}_{hyb} &= \frac{4}{d} \sum_n \langle \alpha\omega_d^n | (\hat{a}^\dagger)^2 \hat{a}^2 | \alpha\omega_d^n \rangle \\ &+ \frac{4}{d} \sum_n \langle \alpha\omega_d^n | \hat{a}^\dagger \hat{a} | \alpha\omega_d^n \rangle - 4 \left(\frac{1}{d} \sum_n \langle \alpha\omega_d^n | \hat{a}^\dagger \hat{a} | \alpha\omega_d^n \rangle \right)^2 \\ &= 4\alpha^4 + 4\alpha^2 - 4\alpha^4 = 4\alpha^2, \end{aligned} \quad (49)$$

which is the same result with coherent states. Second, quantum Fisher information of amplified hybrid states under the photon addition and then subtraction scheme is

$$\begin{aligned} \mathcal{F}_{hyb}^{\hat{a}^{\dagger 2}} &= 4N_{hyb}^{\hat{a}^{\dagger 2}} \left(\frac{1}{d} \sum_n \langle \alpha\omega_d^n | \hat{a}\hat{a}^\dagger (\hat{a}^\dagger)^2 \hat{a}^2 \hat{a}\hat{a}^\dagger | \alpha\omega_d^n \rangle \right) \\ &+ \frac{1}{d} \sum_n \langle \alpha\omega_d^n | \hat{a}\hat{a}^\dagger \hat{a}^\dagger \hat{a} \hat{a}\hat{a}^\dagger | \alpha\omega_d^n \rangle \\ &- 4N_{hyb}^{\hat{a}^{\dagger 2}} \left(\frac{1}{d} \sum_n \langle \alpha\omega_d^n | \hat{a}\hat{a}^\dagger \hat{a}^\dagger \hat{a}\hat{a}^\dagger | \alpha\omega_d^n \rangle \right)^2 \end{aligned} \quad (50)$$

To calculate this, observe that

$$\hat{a}(\hat{a}^\dagger)^3\hat{a}^3\hat{a}^\dagger = (\hat{a}^\dagger)^4\hat{a}^4 + 7(\hat{a}^\dagger)^3\hat{a}^3 + 9(\hat{a}^\dagger)^2\hat{a}^2 \quad (51)$$

$$\hat{a}(\hat{a}^\dagger)^2\hat{a}^2\hat{a}^\dagger = (\hat{a}^\dagger)^3\hat{a}^3 + 5(\hat{a}^\dagger)^2\hat{a}^2 + 4(\hat{a}^\dagger)\hat{a} \quad (52)$$

Therefore, quantum Fisher information is calculated to be

$$\mathcal{F}_{hyb}^{\hat{a}\hat{a}^\dagger} = \frac{4\alpha^2(\alpha^8 + 6\alpha^6 + 14\alpha^4 + 10\alpha^2 + 4)}{(\alpha^4 + 3\alpha^2 + 1)^2}. \quad (53)$$

Third, after $(\hat{a}^\dagger)^2$ to hybrid states, Fisher information is given by

$$\begin{aligned} \mathcal{F}_{hyb}^{\hat{a}^{\dagger 2}} &= 4N_{hyb}^{\hat{a}^{\dagger 2}} \left(\frac{1}{d} \sum_n \langle \alpha\omega_d^n | \hat{a}^2(\hat{a}^\dagger)^2\hat{a}^2(\hat{a}^\dagger)^2 | \alpha\omega_d^n \rangle \right. \\ &+ \frac{1}{d} \sum_n \langle \alpha\omega_d^n | \hat{a}^2\hat{a}^\dagger\hat{a}(\hat{a}^\dagger)^2 | \alpha\omega_d^n \rangle \\ &\left. - 4N_{hyb}^{\hat{a}^{\dagger 2}} \left(\frac{1}{d} \sum_n \langle \alpha\omega_d^n | \hat{a}^2\hat{a}^\dagger\hat{a}(\hat{a}^\dagger)^2 | \alpha\omega_d^n \rangle \right)^2 \right) \quad (54) \end{aligned}$$

To calculate this, observe that

$$\begin{aligned} \hat{a}^2(\hat{a}^\dagger)^2\hat{a}^2(\hat{a}^\dagger)^2 \\ = (\hat{a}^\dagger)^4\hat{a}^4 + 12(\hat{a}^\dagger)^3\hat{a}^3 + 38(\hat{a}^\dagger)^2\hat{a}^2 + 32(\hat{a}^\dagger)\hat{a} + 4 \quad (55) \end{aligned}$$

$$\hat{a}^2(\hat{a}^\dagger)\hat{a}(\hat{a}^\dagger)^2 = (\hat{a}^\dagger)^3\hat{a}^3 + 8(\hat{a}^\dagger)^2\hat{a}^2 + 14(\hat{a}^\dagger)\hat{a} + 4 \quad (56)$$

Therefore, Eq. (54) is calculated to be

$$\mathcal{F}_{hyb}^{\hat{a}^{\dagger 2}} = \frac{4\alpha^2(\alpha^8 + 8\alpha^6 + 24\alpha^4 + 24\alpha^2 + 12)}{(\alpha^4 + 4\alpha^2 + 2)^2}. \quad (57)$$

B. Appendix B

In this appendix, we will compute fidelity and quantum Fisher information of superposition of coherent states, and will not compute gain since it is way too complicated to obtain closed form. First, we calculate the fidelity between the target state and the amplified d -dimensional superposition of coherent states with qudit number k under the photon addition and then subtraction scheme, which is denoted by $F_{SCS}^{\hat{a}\hat{a}^\dagger}$, and under the $(\hat{a}^\dagger)^2$ scheme, which is denoted by $F_{SCS}^{\hat{a}^{\dagger 2}}$, in order.

$$\begin{aligned} F_{SCS}^{\hat{a}\hat{a}^\dagger} &= N_{SCS}^{\hat{a}\hat{a}^\dagger}(\alpha, k, d)^2 N_{k,g\alpha,d}^2 \sum_{m,n} \langle g\alpha\omega_d^m | \omega_d^{km} \hat{a}\hat{a}^\dagger \omega_d^{-kn} | \alpha\omega_d^n \rangle|^2 \\ &= \frac{|\sum_{m,n} (1 + g\alpha^2\omega_d^{(n-m)})\omega_d^{-k(n-m)} \langle g\alpha\omega_d^m | \alpha\omega_d^n \rangle|^2}{d^2(\sum_n \omega_d^{-kn}(\alpha^4\omega_d^{2n} + 3\alpha^2\omega_d^n + 1)\text{Exp}[-\alpha^2(1 - \omega_d^n)])(\sum_n \omega_d^{-kn}\text{Exp}[-g^2\alpha^2(1 - \omega_d^n)])} \\ &= \frac{\{\sum_n (1 + g\alpha^2\omega_d^n)\omega_d^{-kn}\text{Exp}[g\alpha^2\omega_d^n]\}^2}{(\sum_n \omega_d^{-kn}(\alpha^4\omega_d^{2n} + 3\alpha^2\omega_d^n + 1)\text{Exp}[\alpha^2\omega_d^n])(\sum_n \omega_d^{-kn}\text{Exp}[g^2\alpha^2\omega_d^n])}, \quad (58) \end{aligned}$$

$$\begin{aligned} F_{SCS}^{\hat{a}^{\dagger 2}} &= N_{SCS}^{\hat{a}^{\dagger 2}}(\alpha, k, d)^2 N_{k+2,g\alpha,d}^2 \sum_{m,n} \langle g\alpha\omega_d^m | \omega_d^{(k+2)m} \hat{a}^{\dagger 2} \omega_d^{-kn} | \alpha\omega_d^n \rangle|^2 \\ &= \frac{|g^2\alpha^2 \sum_{m,n} \omega_d^{-k(n-m)} \langle g\alpha\omega_d^m | \alpha\omega_d^n \rangle|^2}{d^2(\sum_n \omega_d^{-kn}(\alpha^4\omega_d^{2n} + 4\alpha^2\omega_d^n + 2)\text{Exp}[-\alpha^2(1 - \omega_d^n)])(\sum_n \omega_d^{-(k+2)n}\text{Exp}[-g^2\alpha^2(1 - \omega_d^n)])} \\ &= \frac{g^4\alpha^4 \{\sum_n \omega_d^{-kn}\text{Exp}[g\alpha^2\omega_d^n]\}^2}{(\sum_n \omega_d^{-kn}(\alpha^4\omega_d^{2n} + 4\alpha^2\omega_d^n + 2)\text{Exp}[\alpha^2\omega_d^n])(\sum_n \omega_d^{-(k+2)n}\text{Exp}[g^2\alpha^2\omega_d^n])}, \quad (59) \end{aligned}$$

The two expressions are way too complicated to solve the Eq. (19), thus we will not obtain the closed form of gain.

Second, We calculate quantum Fisher information of the superposition of coherent state with dimension d and

qudit number k , which is denoted by \mathcal{F}_{SCS} , that of amplified superposition of coherent states with dimension d and qudit number k under the photon addition and then subtraction scheme, $\mathcal{F}_{SCS}^{\hat{a}\hat{a}^\dagger}$, and under the $(\hat{a}^\dagger)^2$ scheme, $\mathcal{F}_{SCS}^{\hat{a}^{\dagger 2}}$, in order.

$$\begin{aligned}
\mathcal{F}_{SCS} &= 4N_{k,\alpha,d}^2 \left(\frac{1}{d} \sum_{m,n} \langle \alpha \omega_d^m | \omega_d^{km} (\hat{a}^\dagger)^2 \hat{a}^2 \omega_d^{-kn} | \alpha \omega_d^n \rangle + \frac{1}{d} \sum_{m,n} \langle \alpha \omega_d^m | \omega_d^{km} \hat{a}^\dagger \hat{a} \omega_d^{-kn} | \alpha \omega_d^n \rangle \right) \\
&- 4(N_{k,\alpha,d}^2 \frac{1}{d} \sum_{m,n} \langle \alpha \omega_d^m | \omega_d^{km} \hat{a}^\dagger \hat{a} \omega_d^{-kn} | \alpha \omega_d^n \rangle)^2 = 4N_{k,\alpha,d}^2 \sum_{m,n} (\alpha^4 \omega_d^{2(n-m)} + \alpha^2 \omega_d^{(n-m)}) \omega_d^{-k(n-m)} \text{Exp}[-\alpha(1 - \omega_d^{(n-m)})] \\
&- 4N_{k,\alpha,d}^4 \left(\sum_{m,n} \alpha^2 \omega_d^{(n-m)} \omega_d^{-k(n-m)} \text{Exp}[-\alpha^2(1 - \omega_d^{(n-m)})] \right)^2 \\
&= 4\alpha^2 \frac{\sum_n (\alpha^2 \omega_d^{(2-k)n} + \omega_d^{(1-k)n}) \text{Exp}[\alpha^2 \omega_d^n]}{\sum_n \omega_d^{-kn} \text{Exp}[\alpha^2 \omega_d^n]} - 4\alpha^4 \left(\frac{\sum_n \omega_d^{(1-k)n} \text{Exp}[\alpha^2 \omega_d^n]}{\sum_n \omega_d^{-kn} \text{Exp}[\alpha^2 \omega_d^n]} \right)^2 \tag{60}
\end{aligned}$$

$$\begin{aligned}
\mathcal{F}_{SCS}^{\hat{a}\hat{a}^\dagger} &= 4N_{SCS}^{\hat{a}\hat{a}^\dagger}{}^2 \left(\frac{1}{d} \sum_{m,n} \langle \alpha \omega_d^m | \omega_d^{km} \hat{a}\hat{a}^\dagger (\hat{a}^\dagger)^2 \hat{a}^2 \hat{a}\hat{a}^\dagger \omega_d^{-kn} | \alpha \omega_d^n \rangle + \frac{1}{d} \sum_{m,n} \langle \alpha \omega_d^m | \omega_d^{km} \hat{a}\hat{a}^\dagger \hat{a}^\dagger \hat{a} \hat{a}\hat{a}^\dagger \omega_d^{-kn} | \alpha \omega_d^n \rangle \right) \\
&- 4(N_{k,\alpha,d}^2 \frac{1}{d} \sum_{m,n} \langle \alpha \omega_d^m | \omega_d^{km} \hat{a}\hat{a}^\dagger \hat{a}^\dagger \hat{a} \hat{a}\hat{a}^\dagger \omega_d^{-kn} | \alpha \omega_d^n \rangle)^2 \\
&= 4N_{SCS}^{\hat{a}\hat{a}^\dagger}{}^2 \sum_{m,n} (\alpha^8 \omega_d^{4(n-m)} + 8\alpha^6 \omega_d^{3(n-m)} + 14\alpha^4 \omega_d^{2(n-m)} + 4\alpha^2 \omega_d^{(n-m)}) \omega_d^{-k(n-m)} \text{Exp}[-\alpha(1 - \omega_d^{(n-m)})] \\
&- 4N_{SCS}^{\hat{a}\hat{a}^\dagger}{}^4 \left\{ \sum_{m,n} (\alpha^6 \omega_d^{3(n-m)} + 5\alpha^4 \omega_d^{2(n-m)} + 4\alpha^2 \omega_d^{(n-m)}) \omega_d^{-k(n-m)} \text{Exp}[-\alpha(1 - \omega_d^{(n-m)})] \right\}^2 \\
&= 4 \frac{\sum_n (\alpha^8 \omega_d^{4n} + 8\alpha^6 \omega_d^{3n} + 14\alpha^4 \omega_d^{2n} + 4\alpha^2 \omega_d^n) \text{Exp}[\alpha^2 \omega_d^n] \omega_d^{-kn}}{\sum_n (\alpha^4 \omega_d^{2n} + 3\alpha^2 \omega_d^n + 1) \omega_d^{-kn} \text{Exp}[\alpha^2 \omega_d^n]} - \left(\frac{\sum_n (\alpha^6 \omega_d^{3n} + 5\alpha^4 \omega_d^{2n} + 4\alpha^2 \omega_d^n) \text{Exp}[\alpha^2 \omega_d^n] \omega_d^{-kn}}{\sum_n (\alpha^4 \omega_d^{2n} + 3\alpha^2 \omega_d^n + 1) \omega_d^{-kn} \text{Exp}[\alpha^2 \omega_d^n]} \right)^2 \tag{61}
\end{aligned}$$

$$\begin{aligned}
\mathcal{F}_{SCS}^{\hat{a}^{\dagger 2}} &= 4N_{SCS}^{\hat{a}^{\dagger 2}}{}^2 \left(\frac{1}{d} \sum_{m,n} \langle \alpha \omega_d^m | \omega_d^{km} \hat{a}^2 (\hat{a}^\dagger)^2 \hat{a}^2 \hat{a}^{\dagger 2} \omega_d^{-kn} | \alpha \omega_d^n \rangle + \frac{1}{d} \sum_{m,n} \langle \alpha \omega_d^m | \omega_d^{km} \hat{a}^2 \hat{a}^\dagger \hat{a} \hat{a}^{\dagger 2} \omega_d^{-kn} | \alpha \omega_d^n \rangle \right) \\
&- 4(N_{k,\alpha,d}^2 \frac{1}{d} \sum_{m,n} \langle \alpha \omega_d^m | \omega_d^{km} \hat{a}^2 \hat{a}^\dagger \hat{a} \hat{a}^{\dagger 2} \omega_d^{-kn} | \alpha \omega_d^n \rangle)^2 \\
&= 4N_{SCS}^{\hat{a}^{\dagger 2}}{}^2 \sum_{m,n} (\alpha^8 \omega_d^{4(n-m)} + 13\alpha^6 \omega_d^{3(n-m)} + 46\alpha^4 \omega_d^{2(n-m)} + 46\alpha^2 \omega_d^{(n-m)} + 8) \text{Exp}[-\alpha(1 - \omega_d^{(n-m)})] \omega_d^{-k(n-m)} \\
&- 4N_{SCS}^{\hat{a}^{\dagger 2}}{}^4 \left\{ \sum_{m,n} (\alpha^6 \omega_d^{3(n-m)} + 8\alpha^4 \omega_d^{2(n-m)} + 14\alpha^2 \omega_d^{(n-m)} + 4) \omega_d^{-k(n-m)} \text{Exp}[-\alpha(1 - \omega_d^{(n-m)})] \right\}^2 \\
&= 4 \frac{\sum_n (\alpha^8 \omega_d^{4n} + 13\alpha^6 \omega_d^{3n} + 46\alpha^4 \omega_d^{2n} + 46\alpha^2 \omega_d^n + 8) \text{Exp}[\alpha^2 \omega_d^n] \omega_d^{-kn}}{\sum_n (\alpha^4 \omega_d^{2n} + 4\alpha^2 \omega_d^n + 2) \omega_d^{-kn} \text{Exp}[\alpha^2 \omega_d^n]} \\
&- 4 \left(\frac{\sum_n (\alpha^6 \omega_d^{3n} + 8\alpha^4 \omega_d^{2n} + 14\alpha^2 \omega_d^n + 4) \text{Exp}[\alpha^2 \omega_d^n] \omega_d^{-kn}}{\sum_n (\alpha^4 \omega_d^{2n} + 4\alpha^2 \omega_d^n + 2) \omega_d^{-kn} \text{Exp}[\alpha^2 \omega_d^n]} \right)^2 \tag{62}
\end{aligned}$$